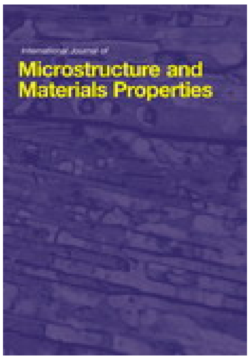

International Journal of Microstructure and Materials Properties

ISSN online: 1741-8429 - ISSN print: 1741-8410
https://www.inderscience.com/ijmmp

High-temperature deformation characteristics of 3D printing of nano-ceramic materials

Xiao Zhang

DOI: 10.1504/IJMMP.2022.10052516

Article History:

Received:	29 June 2022
Accepted:	07 October 2022
Published online:	20 January 2023

High-temperature deformation characteristics of 3D printing of nano-ceramic materials

Xiao Zhang

Institute of Cultural Creative Industry,
Changchun University of Architecture and Civil Engineering,
Changchun, 130000, China
Email: xizhang@mls.sinanet.com

Abstract: In order to improve the application effect of three-dimensional printing of nano ceramic materials, the high-temperature deformation characteristics of three-dimensional printing of nano ceramic materials were studied. First, the main raw materials and experimental instruments for preparing nano ceramic materials were selected. Then, high-temperature nano ceramic materials were prepared by using 8%, 12%, and 15% polyester modified silicone resins respectively; And put it into the storage box of the direct writing 3D printer to print the 3D ceramic sample with the 3D printer. At last, the high temperature deformation characteristics under different high temperature environments are analysed. The results show that the adhesive force and salt spray resistance of 12% polyester modified silicone resin 3D ceramic specimens are good, and the bending strength of 12% polyester modified silicone resin 3D ceramic specimen is high, its structural stability is good, and the deformation value is small under the same high temperature environment.

Keywords: nano-ceramic materials; 3D printing; high-temperature deformation characteristics; densification; bending strength.

Reference to this paper should be made as follows: Zhang, X. (2023) 'High-temperature deformation characteristics of 3D printing of nano-ceramic materials', *Int. J. Microstructure and Materials Properties*, Vol. 16, No. 4, pp.239–251.

Biographical notes: Xiao Zhang received her Master's degree in Design and Art from Jilin University in 2017. Currently, she is a Lecturer at Institute of Cultural Creative Industry, Changchun University of Architecture and Civil Engineering. Her research interests include product design, and cultural and creative product design.

1 Introduction

3D printing technology is a kind of rapid prototyping technology, also known as additive manufacturing technology. With this technology, a target object can be constructed by the layered modelling method through powdered metal and ceramic materials according to the digital model of the target (Li et al., 2019). At present, 3D printing technology has been applied to industrial manufacturing, stomatology and aviation fields, etc. However, during printing of 3D objects with the technology, the ejected nano-ceramic materials continuously superimpose and form at their positions after high-temperature treatment with laser (Zhi et al., 2021), and there will be still residual laser-caused temperature on the surface, which has a certain influence on the formation of nano-ceramic materials and triggers their deformation. Therefore, it is of great significance to study the 3D printing process and the deformation of nano-ceramic materials under the influence of temperature. At present, many scholars study the high-temperature deformation characteristics of nano-ceramic materials. For example, Huamán-Mamani et al. and Wang et al. put forward the analysis method for deformation characteristics of nano-ceramic materials. Huamán-Mamani et al. prepared nano-ceramic materials and then obtained the microstructure of nano-ceramic materials by sintering and analysed their high-temperature deformation characteristics (Huamán-Mamani et al., 2022). Wang et al. (2019) placed the nano-ceramic materials in the high temperature environment, carried on the uniaxial compression treatment to the nano-ceramic materials, and then analysed the elastic deformation state of the materials under the condition of high temperature and compression. They all have obtained the high-temperature deformation characteristics of nano-ceramic materials. However, the experimental environment temperature of the former is lower than the laser temperature during 3D printing, which cannot fully reveal the deformation characteristics of nano-ceramic materials during 3D printing. The latter performs axial compression treatment on nano-ceramic materials at high temperature, which does not occur in the process of 3D printing, so its application range is not wide. In order to solve the problem that the experimental ambient temperature of the existing method is lower than the laser temperature during three-dimensional printing, which cannot fully reveal the deformation characteristics of nano ceramic materials during three-dimensional printing, and the axial compression treatment of nano ceramic materials at high temperature is not widely used, Then, the three-dimensional printer technology to form the final sample layer by layer is used to print the multi-layer grid structure experimental samples. The prepared nano ceramic materials and selected experimental instruments are used to test the heat resistance of the three-dimensional ceramic samples. The corrosion deformation characteristics of the three-dimensional ceramic samples after high temperature treatment are measured by the intelligent salt spray test machine, and the high-temperature deformation characteristics of the nano ceramic materials in the three-dimensional printing process are studied, Provide more accurate attribute data for the application of nano ceramic materials in other fields.

2 High-temperature deformation characteristics of nano-ceramic materials

To detect the high-temperature deformation characteristics of nano-ceramic materials, firstly, the main raw materials for preparing nano-ceramic materials and experimental instruments were selected. Then the materials were prepared according to the preparation process of nano-ceramic materials, and the experimental specimens with multilayer grid structure were printed by direct-writing 3D printer technology. Finally, the heat resistance of 3D ceramic specimens was tested by muffle furnace, so as to detect the high-temperature deformation characteristics of nano-ceramic materials.

2.1 Selection of main raw materials and experimental instruments for nano ceramic materials

The specifications of main raw materials, manufacturers, and proportion and dosage for the preparation of nano-ceramic materials are shown in Table 1.

Table 1 List of main raw materials and dosage for preparation of nano-ceramic materials

Raw material	*Dosage/%*	*Manufacturer*
Silica sol	28	Linyi Zhixuan New Material Co., Ltd.
Siloxane	18	Shanxi Tangyao Biotechnology Co., Ltd.
Polyester modified silicone resin	8/12/15	Suzhou Libo Plastic Technology Co., Ltd.
Copper chromium (black)	12.5	Dongguan Tengda Copper Aluminum Material Co., Ltd.
Glass powder	8	Guilin Lingchuan Xinhua Hui Superfine Powder Factory
Mica powder	6.5	Guilin Lingchuan Xinhua Hui Superfine Powder Factory
Wollastonite fiber	5.5	Tianjin Yandong Mineral Products Co., Ltd.
Alumina whisker	5.5	Beijing Deke Island Technology Co., Ltd.
Dispersant	2	Guangzhou Jianyi Chemical Import and Export Co., Ltd.
Leveling agent	0.5	Guangzhou Jianyi Chemical Import and Export Co., Ltd.

The instruments used in the experiment:

Grinding machine: model: WS-001, manufacturer: Laizhou Shenglong Chemical Machinery Co., Ltd.; Electro- thermostatic blast oven: model: DRP-8804: manufacturer: Suzhou Winson Oven Equipment Co., Ltd.; Electric stirrer: model: S312-120W, manufacturer: Shanghai Yuhua Instrument Equipment Co., Ltd.; Intelligent salt spray tester: model: RK-60, manufacturer: Hebi Ruike Instrument Co., Ltd.; High-temperature muffle furnace: model: XD-horizontal, manufacturer: Luoyang Xingding Kiln Co., Ltd.; Electronic balance: model: BSA224S, manufacturer: Henan Gansi Biotechnology Co., Ltd.; Adhesion tester, model: TC10, manufacturer: Times Top Instrument Co., Ltd.

2.2 Preparation of nano ceramic materials

The components of nano-ceramic materials in Table 1 were proportionally weighed by an electronic balance, in which the addition amount of polyester modified silicone resin was 8%, 12% and 15%, respectively. Three contents of polyester modified silicone resin were added to three appropriate dispersion containers (Hw et al., 2020; Zhao et al., 2019; Deryugin et al., 2019). The rotational speed of the dispersion containers was set to 600 r/min, and dispersants, fillers and copper chromium (black) were respectively added to the dispersion containers in order. After 20-min stirring with a stirrer, the nano-ceramic mixed liquid was poured into a sand mill, and a nano-ceramic colour paste with fineness less than 30 μm was obtained after 40-min grinding with a sand mill. After the nano-ceramic colour paste was placed at room temperature for 3.5 h, siloxane, silica sol and leveling agent were sequentially added into it (Besharatloo et al., 2019; Goulmy et al., 2021; Zhang et al., 2021), and then stirred for 35min by a stirrer to obtain a uniformly dispersed nano-ceramic mixed colour paste. Then, the large particles in the nano-ceramic mixed colour paste were filtered by 150-mesh spun silk to obtain high-temperature nano-ceramic materials which can be used for 3D printing. Using the above-mentioned nano-ceramic material preparation process, several specimens of high-temperature nano-ceramic materials with different addition amounts of polyester modified silicone resin were made, and the high-temperature nano-ceramic materials were marked as H-8, H-12 and H-15 for later use according to the addition amounts of polyester modified silicone resin.

2.3 Preparation of 3D printed ceramic specimens with multi-layer grid structure

Using the direct-writing 3D printer technology, experimental specimens with multi-layer grid structure were printed. The direct-writing 3D printing technology is a technology that decomposes a three-dimensional specimen into a two-dimensional planar structure (Maeda et al., 2019; Curcio et al., 2019), and then form the final specimen by superimposing it layer by layer. The structure of the direct-writing3D printer is shown in Figure 1.

Figure 1 Structure diagram of direct writing 3D printer (see online version for colours)

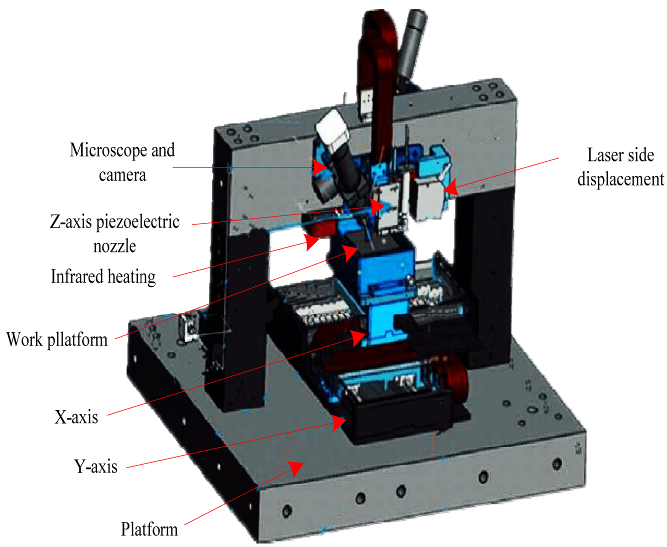

The workbench of the direct-writing 3D printer can move left and right horizontally, and its nozzle can move up and down. The high-temperature nano-ceramic materials prepared in the last section were poured into the printer storage box, and then the printing table was adjusted to the horizontal state (Yw et al., 2022). The moving speed of the nozzle of the 3D printer to the left and right directions was set at 2.5 mm/s and the printing pressure was set at 9 MPa. After conductive silver ink was uniformly coated on the PI film, the first conductive rectangular electrode grid was obtained. Then the nozzle of 3D printer was used to spray the high-temperature nano-ceramic materials into the first conductive rectangular electrode grid according to its mathematical model parameters, and the second conductive electrode grid was obtained after spraying (Quan et al., 2020). After spraying of high-temperature nano-ceramic materials layer by layer according to this step, 3D ceramic specimens with different contents of polyester modified silicone resin were obtained.

2.4 Testing and analysis method of high temperature deformation characteristics of three-dimensional ceramic samples

After the ceramic specimens with different contents of polyester modified silicone resin were obtained by a direct-writing 3D printer, the heat resistance of the 3D ceramic specimens was tested by a muffle furnace. The 3D ceramic specimens were placed in a muffle furnace with temperature raised to 950°C and kept for 8 h, and then the high-temperature deformation state of 3D ceramic specimen was observed. The intelligent salt spray tester was used to detect the corrosion deformation characteristics of 3D ceramic specimens after high-temperature treatment. In order to ensure the validity of the experimental results, the 3D ceramic specimens after high-temperature treatment in a muffle furnace were quenched. The 3D ceramic specimens taken out of the muffle furnace were soaked in tap water at room temperature for 15min, and after full cooling, they were put into the muffle furnace again for high-temperature treatment. After three cycles, the high-temperature deformation characteristics of the 3D ceramic specimens were tested.

The grain size and densification of 3D ceramic specimens are the key factors that affect their deformation at high temperature (Zhuo et al., 2019). Under consideration of the grain size and densification of 3D ceramic specimens, the bending strength of ceramic specimens during high-temperature deformation was calculated, and its expression formulas are shown in equations (1) and (2):

$$\kappa_f = \kappa_0 \exp(-np) \tag{1}$$

$$\kappa_f' = \kappa_0' + \beta d^{-1/2} \tag{2}$$

where κ_f and κ_f', respectively, represent the deformation bending strength of a 3D ceramic specimen affected by grain size and densification; σ_f' represents a constant between 3–8; p represents the porosity of the 3D ceramic specimen; σ_0 presents the strength of 3D ceramic specimen when it is completely compact; σ_0' represents the strength of the 3D ceramic specimen in infinite single crystal; β and d, respectively, represent the influence coefficient and grain diameter.

To sum up, with prepared nano-ceramic materials and selected experimental instruments, the corrosion deformation characteristics of 3D ceramic specimens after high-temperature treatment are determined using an intelligent salt spray testing machine, thus detecting the high-temperature deformation characteristics of nano-ceramic materials.

3 Experimental analysis

With the prepared 3D ceramic specimens H-8, H-12 and H-15 as experimental objects, the high-temperature deformation characteristics were analysed by the method of high-temperature deformation characteristics detection and analysis proposed in this paper. The method has been described in detail in the above research, and it is only briefly introduced here.

3.1 Adhesion test

The 3D ceramic specimens H-8, H-12 and H-15 were put into a muffle furnace with temperature set to 800°C for 30h, and the adhesion detector was adopted to detect the adhesion of the 3D ceramic specimens at different high temperatures. The results are shown in Table 2.

Table 2 Adhesion test results of polyester modified silicone resin with different contents (MPA)

High temperature time/h	*H–8*	*H–12*	*H–15*
2	5.42	5.46	6.01
4	5.42	5.46	6.01
6	5.42	5.46	6.01
8	5.41	5.46	6.01
10	5.41	5.46	5.94
12	5.41	5.45	5.92
14	5.39	5.45	5.89
16	5.39	5.45	5.77
18	5.37	5.43	5.73
20	5.36	5.42	5.62
22	5.34	5.41	5.54
24	5.34	5.39	5.50
26	5.32	5.39	5.46
28	5.31	5.36	5.43
30	5.31	5.36	5.39

From Table 2, it can be seen that the adhesion of 3D ceramic specimens added with different contents of polyester modified silicone resin decreases with the increase of high temperature duration, and when the high temperature time lasts for about 8 h, the adhesion value remains the initial value and is not affected by high temperature. When the high temperature time exceeds 8 h and 10 h respectively, the adhesion of 3D ceramic specimens with different contents of polyester modified silicone resin gradually shows a decreasing trend. Among them, the adhesion values of 3D ceramic specimens with 8% and 12% polyester modified silicone resin are not much different, and the extent of their decrease with high temperature is slightly small. Although the adhesion of the 3D ceramic specimen with 15% polyester modified silicone resin is always high, it decreases significantly after the high temperature lasts more than 10 h. The result shows that the ceramic edge of the 3D ceramic specimen is easy to peel off under the influence of high temperature, which affects its overall adhesion and is prone to cause deformation. To sum up, the 3D ceramic specimens with 8% and 12% polyester modified silicone resin, separately, has good adhesion, and they are not easy to deform at high temperature.

3.2 Salt spray resistance test

The intelligent salt spray tester was used to test the salt spray properties of 3D ceramic specimens with different contents of polyester modified silicone resin in different high temperature environments. The results are shown in Table 3.

Table 3 Salt spray test results of 3D ceramic specimens of polyester modified silicone resin with different contents (H)

Temperature/℃	*H–8*	*H–12*	*H–15*
800	654	663	664
820	651	659	651
840	646	651	646
860	639	647	635
880	624	638	627
900	603	618	604
920	592	603	588
940	577	598	562
960	550	572	544
980	543	559	525
1000	521	530	507
1020	501	521	490
1040	486	499	463
1060	461	473	431
1080	422	454	399

From Table 3, it can be seen that the salt spray time of 3D ceramic specimens with different contents of polyester modified silicone resin is inversely proportional to the temperature. Before the high temperature of 920°C, the salt spray time of 3D ceramic specimens with different contents of polyester modified silicone resin decreases slightly. When the high temperature exceeds 920°C, the salt spray time of 3D ceramic specimens with different contents of polyester modified silicone resin decreases relatively largely. Before the high temperature of 920°C, the salt spray time of 3D ceramic specimens with 8%, 12% and 15% polyester modified silicone resin, respectively, has little difference. However, with the increase of high temperature, the salt spray time of 3D ceramic specimens with 15% polyester modified silicone resin decreases rapidly, which indicates that corrosion deformation is easy to occur in high temperature and salt spray environment.

3.3 Analysis of high-temperature stress characteristics

Stress was used as an index to measure the deformation characteristics of 3D ceramic specimen with different polyester modified silicone resin contents, and the deformation stress changes of 3D ceramic specimens at different temperature and time were tested. The results are shown in Figure 2.

Figure 2 High-temperature stress transformation of 3D ceramic specimen modified by polyester with different content (see online version for colours)

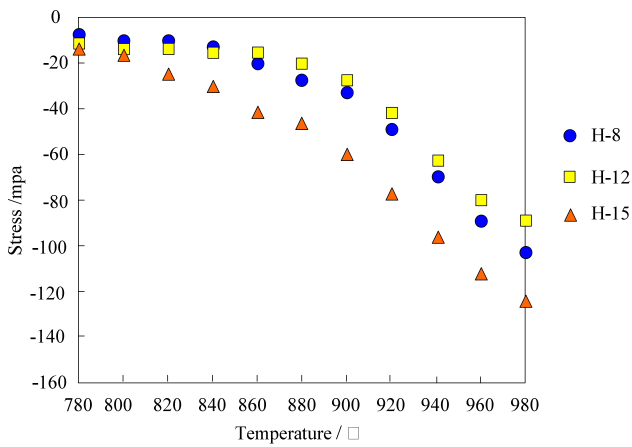

According to Figure 2, the high-temperature stress of 3D ceramic specimens with different polyester modified silicone resin contents are greatly influenced by the ambient temperature, and the higher the ambient temperature, the greater the stress change of 3D ceramic specimens. Before the ambient temperature of 800°C, the high-temperature stress of 3D ceramic specimens with different polyester modified silicone resin is almost the same, but with the increase of ambient temperature, the high-temperature stress of 3D ceramic specimens with 15% polyester modified silicone resin show a slightly decreasing trend. However, the high-temperature stress of 3D ceramic specimens with 8% and 12% polyester modified silicone resin are similar before the ambient temperature of 860°C. When the ambient temperature exceeds 860°C, the high-temperature stress of 3D ceramic specimen with 12% polyester modified silicone resin is higher than that of 3D ceramic specimen with 8% polyester modified silicone resin. In conclusion, under higher ambient temperature, the stress of 3D ceramic specimens is greater, and the deformation stress of 3D ceramic specimen with 12% polyester modified silicone resin in high temperature environment is small, which indicates that 3D ceramic specimens with 12% polyester modified silicone resin are stronger and less prone to deformation. This is because the three-dimensional ceramic samples after high temperature treatment in muffle furnace are quenched by this method.

3.4 Deformation analysis of 3D ceramic specimens under different conditions

The deformation of 3D ceramic specimens in high temperature environment was analysed from the point of densification. The high-temperature environment was set at

800°C for 30 h to analyse the densification change of 3D ceramic specimens with different contents of polyester modified silicone resin. The results are shown in Figure 3.

Figure 3 Densification changes of 3D ceramic specimens under high temperature environment: (a) H-8; (b) H-12 and (c) H-15 (see online version for colours)

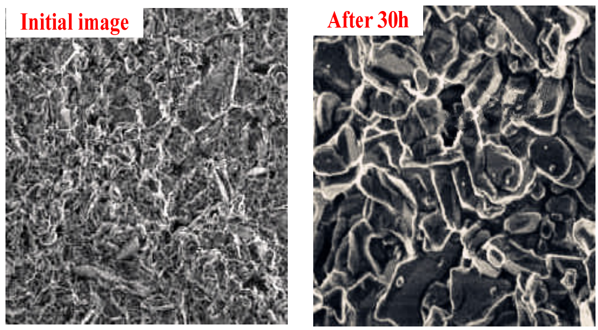

(a)

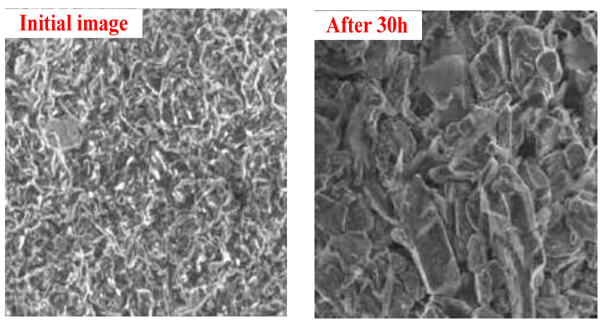

(b)

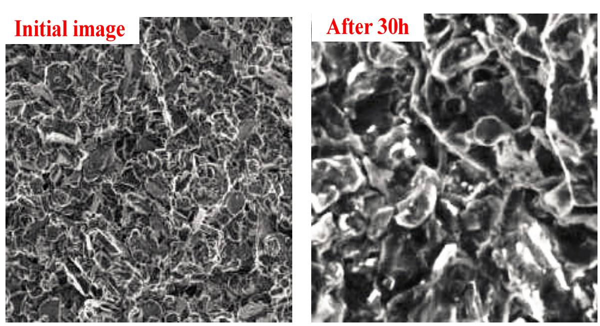

(c)

According to Figure 3, the densification of 3D ceramic specimens with different contents of polyester modified silicone resin is different, and the densification of 3D ceramic specimens changes greatly under high temperature environment. Among them, the densification of the binder in the initial image of the 3D ceramic specimens with 8% and 15% polyester modified silicone resin is slightly higher. After 30 h of high-temperature treatment, the densification of the binder of the 3D ceramic specimen becomes larger, and large black holes appear among the binder, which indicates that the 3Dceramic specimens with 8% and 15% polyester modified silicone resin are affected by high temperature, and their internal structure become fragile, so they are easy to deform under pressing by 3D printing. However, the densification of the binder in the initial image of 3D ceramic specimen with 12% polyester modified silicone resin and the densification of the binder after 30-h high-temperature treatment are both small, so it is not easy to deform. To sum up, the smaller the densification of 3D ceramic specimen, the less likely it is to be deformed.

According to the grain morphology of 3D printed specimens, the deformation state of 3D ceramic specimens with different contents of polyester modified silicone resin at high temperature was analysed, and the grain morphology of 3D ceramic specimens after 30 h of high-temperature treatment was given. The results are shown in Figure 4.

Figure 4 Grain morphology of 3D ceramic specimens of polyester modified silicone resin with different content after high-temperature treatment

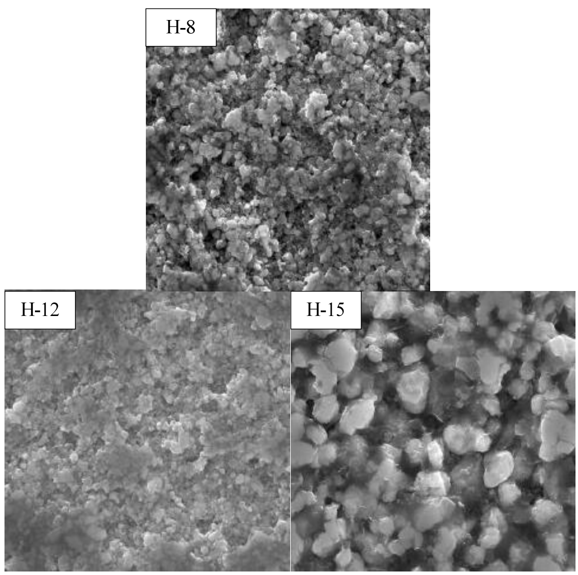

According to the analysis of Figure 4, after 30-h high-temperature treatment, the grains of 3D ceramic specimens with 8% and 15% polyester modified silicone resin are coarsened, especially the grains of 3D ceramic specimens with 15% polyester modified silicone resin. After coarsening, only tiny grain structures remain, which reduce the supporting force of 3D ceramic specimens and make the deformation of 3D ceramic specimens more serious. However, after 30 h of high-temperature treatment, the grain surface morphology of the 3D ceramic specimen with 12% polyester modified silicone resin changes little, which make the 3D ceramic specimens difficult to deform at high temperature.

With the bending strength at high temperature as an index to measure the deformation of 3D ceramic specimens, the bending strength of 3D ceramic specimens with different contents of polyester modified silicone resin at different temperatures was tested. The results are shown in Figure 5.

Figure 5 Changes in bending strength of 3D ceramic specimens at different temperatures

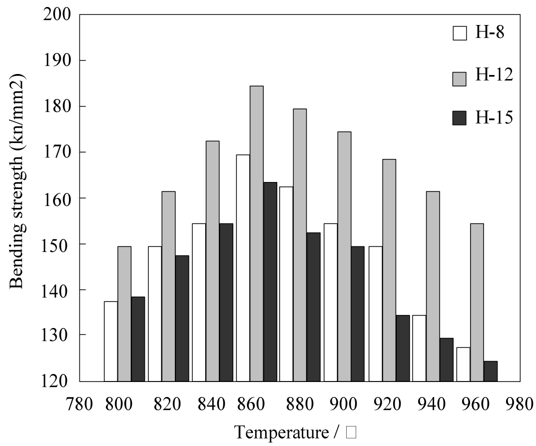

From the analysis of Figure 5, it can be seen that the bending strength of 3D ceramic specimens with different contents of polyester modified silicone resin shows a peak distribution with the increase of ambient temperature. Among them, the 3D ceramic specimen with 12% polyester modified silicone resin has the highest bending strength at the same temperature, which indicates that the 3D ceramic specimen is slightly deformed at high temperature. The bending strength of 3D ceramic specimen with 15% polyester modified silicone resin is the lowest at the same temperature, which indicates that the 3D ceramic specimen is not easy to deform at high temperature. The main reason is that the three-dimensional sample is decomposed into two-dimensional planar structure, and then the three-dimensional printer technology is used to print the multi-layer grid structure experimental sample.

4 Conclusion

In order to solve the problem of deformation of nano ceramic materials after laser high-temperature treatment, the high-temperature deformation characteristics of nano ceramic materials in three-dimensional printing were studied. First, the main raw materials and experimental instruments for preparing nano ceramic materials were selected. Then the materials were prepared according to the preparation process of nano ceramic materials, and the experimental samples with multi-layer grid structure were printed by direct writing three-dimensional printing technology. Finally, the heat resistance of three-dimensional ceramic samples was tested by muffle furnace to detect the high-temperature deformation characteristics of nano ceramic materials. The results show that under the same high temperature environment, the deformation characteristics of the three-dimensional ceramic samples with different content of polyester modified silicone resin are different, and the deformation of the three-dimensional ceramic samples with 12% polyester modified silicone resin is least affected by the high temperature environment. In addition, the densification degree and grain size of three-dimensional ceramic samples are different under the same high temperature environment. It can provide accurate data for the application of nano ceramic materials in other fields. In the future development, the performance of nano ceramic materials in other fields will be analysed.

Acknowledgements

This project is funded by the Education Department of Jilin Province, the project is: Design and development of snow and ice tourism Products (Souvenirs) in Jilin Province, no. JJKH20211427SK.

References

Besharatloo, H., Nicolás, M.D., Roa, J.J., Dios, M. and Llanes, L. (2019) 'Assessment of mechanical properties at microstructural length scale of Ti(c, n)–feni ceramic-metal composites by means of massive nanoindentation and statistical analysis', *Ceramics International*, Vol. 45, No. 16, pp.20202–20210.

Curcio, M., Stefanis, A.D., Bonis, A.D., Teghil, R. and Rau, J.V. (2019) 'Pulsed laser deposited bioactive RKKP-MN glass-ceramic coatings on titanium', *Surface and Coatings Technology*, Vol. 357, pp.122–128.

Deryugin, E.E., Schmauder, S., Panin, V.E., Eremin, M.O. and Kvashnina, O.S. (2019) 'Study of deformation and fracture of ZrO2+3%Y2O3 ceramics by wedge splitting of a chevron-notched specimen', *Engineering Fracture Mechanics*, Vol. 218, p.106573.

Goulmy, J.P., Camus, G. and Rebillat, F. (2021) 'Monitoring damage evolution of ceramic matrix composites during tensile tests using electrical resistivity: crack density-based electromechanical model', *Journal of the European Ceramic Society*, Vol. 41, No. 1, pp.121–129.

Huamán-Mamani, F.A., Jiménez-Holgado, C. and Jiménez-Melendo, M. (2022) 'Fabrication, microstructure and high-temperature plastic deformation of three-phase Al_2O_3/Er_3 Al_5 O_{12}/ZrO_2 sintered ceramics', *Ceramics International*, Vol. 48, No. 2, pp.2012–2020.

Hw, A., Fld, A., Zj, A., Xi, C.A., Zhi, Y.A., Yz, A. and Chen, K.L. (2020) 'Electrical insulation improvements of ceramic coating for high temperature sensors embedded on aeroengine turbine blade', *Ceramics International*, Vol. 46, No. 3, pp.3600–3605.

Li, Z., Zhang, F., Luo, X. and Cai, Y. (2019) 'Fundamental understanding of the deformation mechanism and corresponding behavior of Rb-SiC ceramics subjected to nano-scratch in ambient temperature', *Applied Surface Science*, Vol. 469, 1 March, pp.674–683.

Maeda, K., Iwasaki, K., Urata, S., Akatsuka, K. and Yasumori, A. (2019) '3d microstructure and crack pathways of toughened CaO–Al_2O_3–SiO2 glass by precipitation of hexagonal $CaAl_2Si_2O_8$ crystal', *Journal of the American Ceramic Society*, Vol. 102, No. 9, pp.5535–5544.

Quan, Z., Xiang, D.D., Jha, B., Jya, B., Xza, B., Yda, B. and Hong, D. (2020) 'High strength aligned sic nanowire reinforced SiC porous ceramics fabricated by 3D printing and chemical vapor infiltration', *Ceramics International*, Vol. 46, No. 5, pp.6978–6983.

Wang, Z., Li, R. and Song, W. (2019) 'Dynamic failure and inelastic deformation behavior of sic ceramic under uniaxial compression', *Ceramics International*, Vol. 46, No. 1, pp.169–183.

Yw, A., Yc, A., Yc, B., Rong, W.B. and Zp, A. (2022) 'Lattice-structured sic ceramics obtained via 3D printing, gel casting, and gaseous silicon infiltration sintering', *Ceramics International*, Vol. 48, No. 5, pp.6488–6496.

Zhang, X., Yuan, J., Ding, Y., Liu, B. and Yang, J. (2021) 'Directly growing nanowire-assembled nanofibrous ceramic foams with multi-lamellar structure via freeze-casting process', *Journal of the European Ceramic Society*, Vol. 41, No. 1, pp.1041–1047.

Zhao, Y., Yu, T., Guan, C., Sun, J. and Tan, X. (2019) 'Microstructure and friction coefficient of ceramic (tic, tin and b4c) reinforced Ni-based coating by laser cladding', *Ceramics International*, Vol. 45, No. 16, pp.20824–20836.

Zhi, Z.A., Jzb, C., Myb, C., Wen, Y., Zhe, Q., Xian, W.D., Chen, K. and Liu, Q.C. (2021) 'High-temperature thermal expansion behaviour of c/SiC studied using an in-situ optical visualisation method and numerical simulations in a quartz lamp array heating environment – Sciencedirect', *Ceramics International*, Vol. 47, No. 9, pp.12547–12556.

Zhuo, T.A., Yy, A., Yong, W.B., Hw, A., Wei, L.A. and Sw, A. (2019) 'Fabrication and properties of a high porosity H – Bn–SiO_2 ceramics fabricated by stereolithography-based 3d printing', *Materials Letters*, Vol. 236, pp.144–147.